Macromolecules
ARTICLE

Macromolecules **2010**, *43*, 8559–8569 **8559**
DOI: 10.1021/ma101543d

A New Mesophase of Isotactic Polypropylene in Copolymers of Propylene with Long Branched Comonomers

Claudio De Rosa,* Finizia Auriemma, Rocco Di Girolamo, Luisa Romano, and Mattia Roberto De Luca

Dipartimento di Chimica "Paolo Corradini", Università di Napoli "Federico II", Complesso Monte S.Angelo, Via Cintia, I-80126 Napoli, Italy

Received July 9, 2010; Revised Manuscript Received September 2, 2010

ABSTRACT: Isotactic propylene−1-octene (iPPC8) and propylene−1-octadecene (iPPC18) copolymers have been synthesized with a highly isospecific C_2-symmetric metallocene catalyst. iPPC8 copolymers crystallize in the α form of iPP for octene concentration up to 12−13 mol %, whereas iPPC18 copolymers crystallize in the α form for very low octadecene concentration and in a new mesomorphic form for octadecene contents higher than 2−3 mol %. In both copolymers crystals of α form transform into the new mesophase by stretching at high deformations. This mesophase is different from the quenched mesomorphic form of the iPP homopolymer. In fact, the diffraction patterns of the new mesophase of iPPC18 copolymers present a strong equatorial reflection at $2\theta = 20°$, which is absent in the diffraction pattern of the mesophase of iPP. The new mesophase is characterized by parallel chains in 3/1 helical conformation packed at average interchain distances of about 6 Å, defined by the self-organization of the flexible side groups, and high degree of disorder in the lateral packing of the chains.

Introduction

Samples of isotactic polypropylene (iPP) and of copolymers of propene with other 1-olefins prepared with single-center metallocene catalysts have shown crystallization behavior and mechanical properties different from the properties of analogous samples prepared with Ziegler−Natta catalysts. Extensive investigations have been focused on the study of the influence of the presence of comonomeric units on the crystallization of α and γ forms of iPP and on the mechanical properties.[1−34] These metallocene-based iPP copolymers are more chemically homogeneous than the samples prepared with Ziegler−Natta catalysts and show low levels of solubles even at relatively high comonomer incorporation. Moreover, metallocene catalysts afford incorporation of large contents of comonomer, copolymerization of cyclic and other comonomer types that are not easily incorporated with classical Ziegler−Natta catalysts, and excellent control of stereoregularity. In addition, they may yield copolymers with a truly random comonomer distribution, uniform intermolecular distribution of the comonomer content, and narrow molecular weight distribution.

To date, metallocene-based propylene copolymers have been synthesized with a variety of comonomers (ethylene, butene, hexene, octene, etc.), giving a wide range of interesting materials.[1−34] These characteristics of metallocene-based iPP copolymers have allowed studying the effects of different comonomers on the crystallization of α and γ forms of iPP[2−4,8−10,14,15,26,29] and on the mechanical properties[19−23,27,30,32] and, more recently, discriminating between the influences of stereo defects (for instance, *rr* triad defects) and constitutional defects on the crystallization behavior and material properties.[26,27,29,30]

Copolymers with ethylene, butene, hexene, and octene comonomeric units show decrease of melting temperature and crystallinity and great enhancement of ductility, flexibility, and toughness compared to highly stereoregular iPP, but with important differences in the values of elastic modulus and strength depending on the comonomer and on the contemporarily presence of stereo and regio defects.[27] The different mechanical behavior is related to the different degrees of inclusion of stereo defects and constitutional defects in the crystals of α and γ forms of iPP and differences in the partitioning of defects between crystals of α and γ forms. This results in a different degree of disturbance of crystals with formation of more or less defective crystals, even for similar values of degree of crystallinity.[27,30]

These properties are related to the structure, the crystal morphology, and the polymorphic transitions occurring during stretching, which are all affected by the presence of comonomers. For copolymers with butene and hexene units, crystals of α and γ forms present in the unstretched compression-molded film transform by stretching into the mesomorphic form,[27,30] which facilitates successive further deformation of the sample up to very high strains, resulting in highly flexible materials. The transformation of α or γ forms into the mesomorphic form by stretching has also been observed in stereodefective iPP homopolymer samples containing high concentration of *rr* triad stereo defects (higher than 5−6 mol %).[35,36] It has been suggested that this transition occurs through the destruction of the lamellar crystals by pulling chains out from the original crystals and successive reorganization of chains in crystalline aggregates of the mesomorphic form,[37] which is characterized by bundles of parallel chains in 3/1 helical conformation and small order in the lateral packing.[38] Moreover, it has been argued that the replacement of monoclinic lamellae and a spherulitic superstructure by randomly arranged isometric nodules of the mesophase leads to a distinct increase of the ductility and toughness.[39]

Studies of copolymers of propylene with long branched α-olefins (from 1-octene to 1-octadecene) are less frequent.[2,9,12,13,18,19,21] For copolymers with 1-octadecene a considerable decrease of crystallinity with comonomer content is observed, and at high

*To whom correspondence should be addressed: Tel ++39 081 674346; Fax ++39 081 674090; e-mail claudio.derosa@unina.it.

Published on Web 09/30/2010

Chart 1. Structure of the Metallocene Complex Dimethylsilyl-2,2′-dimethyl-4,4′-diphenylindenile Zirconium Dichloride, $Me_2Si(2\text{-}Me\text{-}4\text{-}Ph\text{-}Ind)_2ZrCl_2$, Used as Catalysts for the Preparation of iPPC8 and iPPC18 Copolymer Samples

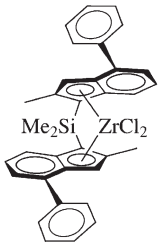

comonomer concentration a transformation of the α form into mesomorphic-like ordered entities has been observed.[21] Moreover, the crystallite morphology changes from almost perfect spherulites to bundlelike crystals. All these variations in crystal structure (number, size, and perfection of crystallites, crystal lattice, and morphological details) significantly influence the mechanical behavior of these copolymers, with decrease of rigidity and impact strength and increase of ductility with increasing comonomer content.[21]

In this paper we report a study of the structures of copolymers of iPP with 1-octene (iPPC8) and 1-octadecene (iPPC18) comonomers in powder melt-crystallized samples and in fiber specimens, aimed at demonstrating that in these copolymers a new mesomorphic form crystallizes at high comonomer concentrations. This new mesophase crystallizes already in the powder samples without quenching and stretching and is different from the well-known mesophase of iPP that normally is obtained by quenching the melt or by stretching at high deformations.

Experimental Section

The iPP homopolymer sample and propene−1-octene (iPPC8) and propene−1-octadecene (iPPC18) copolymer samples have been prepared at a temperature of 25 °C with the C_2-symmetric metallocene catalyst, shown in Chart 1. The catalyst precursor is the metallocene complex dimethylsilyl-2,2′-dimethyl-4,4′-diphenylindenile zirconium dichloride, $Me_2Si(2\text{-}Me\text{-}4\text{-}Ph\text{-}Ind)_2ZrCl_2$, which is activated with methylalumoxane (MAO). The C_2-symmetric metallocene of Chart 1 is highly isospecific but not completely regioselective and produces highly isotactic iPP homopolymer sample, containing no detectable *rr* triad stereo defects and only very small amount (about 0.2 mol %) of regio defects due to the presence of secondary 2,1 propene units.

All copolymerizations were run at 25 °C in a 250 mL Pyrex reactor, agitated with magnetic stirrer, containing toluene (100 mL), MAO (1.5 mL), and liquid 1-octene (C8) or 1-octadecene (C18). All procedures were conducted in an argon atmosphere, and the residual inert gas was removed up to a final vacuum pressure of 15 mbar. Propene was bubbled through the liquid phase at pressure of 2.5 bar. The polymerization was started by syringing into the reactor a toluene solution of the catalyst (2−3 mg), and the Al/Zr molar ratio was maintained at about 1000. The polymerization was stopped when the propene pressure decreases at 2.3 bar. Under such conditions, total monomer conversions were lower than 10%, ensuring a nearly constant feeding ratio. The copolymers were coagulated with excess methanol acidified with enough HCl(aq, conc) to prevent the precipitation of alumina from MAO hydrolysis, filtered, washed with further methanol, and vacuum-dried. Typical yields were 2−3 g. All the synthesized copolymer samples are listed in Table 1.

The microstructural data of all samples have been obtained from ^{13}C NMR analysis. All spectra were obtained using a Bruker DPX-400 spectrometer operating in the Fourier transform mode at 120 °C at 100.61 MHz. The samples were dissolved with a 8% w/v concentration in 1,1,2,2-tetrachloroethane-d_2 at 120 °C. The carbon spectra were acquired with a 90° pulse and 12 s of delay between pulses and CPD (WALTZ 16) to remove $^1H-^{13}C$ coupling. About 1500−3000 transients were stored in 32K data points using a spectral window of 6000 Hz. For the iPP sample, the peak of the *mmmm* pentad in the ^{13}C spectra (21.8 ppm) was used as a reference. For copolymers, the peak of the propylene methine carbon atoms was used as internal reference at 28.83 ppm. The resonances in the spectra of iPPC8 and iPPC18 copolymers were assigned according to refs 40−42, and the 1-octene or 1-octadecene concentrations in the copolymers were determined from the constitutional diads PP, PX, XX distribution (P = propene, X = octene or octadecene). The NMR data also indicate that all copolymer samples have a random distribution of comonomers and homogeneous intermolecular composition.

The calorimetric measurements were performed with a differential scanning calorimeter (DSC) Mettler DSC-30 in a flowing N_2 atmosphere.

Films used for the X-ray fiber diffraction characterization have been prepared by compression-molding. Powder samples have been heated at temperatures higher than the melting temperatures under a press at low pressure and slowly cooled to room temperature. Oriented fibers of the copolymer samples have been obtained by stretching at room temperature compression-molded films.

X-ray diffraction patterns were obtained with Ni filtered Cu Kα radiation. The powder profiles were obtained with an automatic Philips diffractometer, whereas the fiber diffraction patterns were recorded on a BAS-MS imaging plate (FUJIFILM) using a cylindrical camera and processed with a digital imaging reader (FUJIBAS 1800).

The indices of crystallinity (x_c) were evaluated from the X-ray powder diffraction profiles by the ratio between the crystalline diffraction area (A_c) and the total area of the diffraction profile (A_t), $x_c = A_c/A_t$. For the iPP homopolymer sample and for the iPPC8 and iPPC18 copolymer samples with low comonomer concentration, the amorphous halo has been obtained from the X-ray diffraction profile of an atactic polypropylene. For iPPC8 copolymer samples with higher octene concentration the amorphous halo has been obtained from the X-ray diffraction profile of the amorphous sample iPPC8-6 with the highest octene concentration (15.9 mol %). For iPPC18 copolymer samples with high octadecene concentration (samples iPPC18-3, iPPC18-4, and iPPC18-5), the amorphous halos have been obtained from the X-ray diffraction profiles of the same samples in the melt state recorded at temperatures higher than the corresponding melting temperatures and extrapolating the 2θ position of the maxima of the diffuse scattering to room temperature. The amorphous scattering was then scaled and subtracted from the X-ray diffraction profiles of the semicrystalline samples to obtain the crystalline diffraction area.

Densities of the copolymer samples were measured by flotation of compression-molded films at 25 °C in solutions of water and ethyl alcohol.

Results and Discussion

The highly isoselective C_2-symmetric metallocene of Chart 1 produces high molecular mass and highly stereoregular iPP homopolymer and iPPC8 and iPPC18 copolymers. In fact, the concentration of *rr* triad stereo errors is below the limit detectable by the ^{13}CNMR (lower than 0.01%), whereas a very small amount of regio defects, due to secondary 2,1-erythro (2,1e) insertions of propylene units (nearly 0.2 mol %), has been identified from the ^{13}C NMR spectra.

The X-ray powder diffraction profiles of as-prepared (precipitated form the polymerization solution) and melt-crystallized samples of iPPC8 and iPPC18 copolymers, compared with those of the iPP homopolymer sample (iPP-25), are reported in

Table 1. Conditions of Polymerization, Composition (mol % and wt % C8 or C18), and Melting Temperature of As-Prepared Samples (T_m) of Samples of iPPC8 and iPPC18 Copolymers Prepared with the Catalyst of Chart 1, $Me_2Si(2\text{-Me-4-Ph-Ind})_2ZrCl_2$/MAO[a]

sample	comonomer	feed composition (mL C8 or C18)	composition (mol % C8 or C18)[b]	composition (wt % C8 or C18)	weight polymer (g)	T_m (°C)[c]
iPP-25		0	0	0	1.33	160
iPPC8-1	1-octene	1	1.9	4.9	2.37	132.5
iPPC8-2	1-octene	4	4.3	10.1	1.76	114.4
iPPC8-3	1-octene	6	7.1	16.9	2.16	91.8
iPPC8-4	1-octene	2	10.3	23.4	1.7	72.6/53.2
iPPC8-5	1-octene	8	12.8	28.1	1.39	47.3
iPPC8-6	1-octene	10	15.9	33.5	1.45	44.9
iPPC18-1	1-octadecene	2	0.8	4.6	1.3	133
iPPC18-2	1-octadecene	4	1.3	7.3	1.8	115.5
iPPC18-3	1-octadecene	8	2.8	14.7	2.4	85
iPPC18-4	1-octadecene	10	3.9	19.6	3.3	78.5
iPPC18-5	1-octadecene	15	8.1	34.6	3.8	51.3

[a] Polymerization temperature $T = 25$ °C, initial pressure of propylene in the reactor $P = 2.5$ bar, solvent: toluene (100 mL), volume reactor: 250 mL, volume MAO = 1.5 mL, conversion lower than 10%. [b] Determined from solution ^{13}C NMR analysis. [c] Melting temperatures of as-prepared samples from DSC scans at heating rate of 10 °C/min (Figure 3).

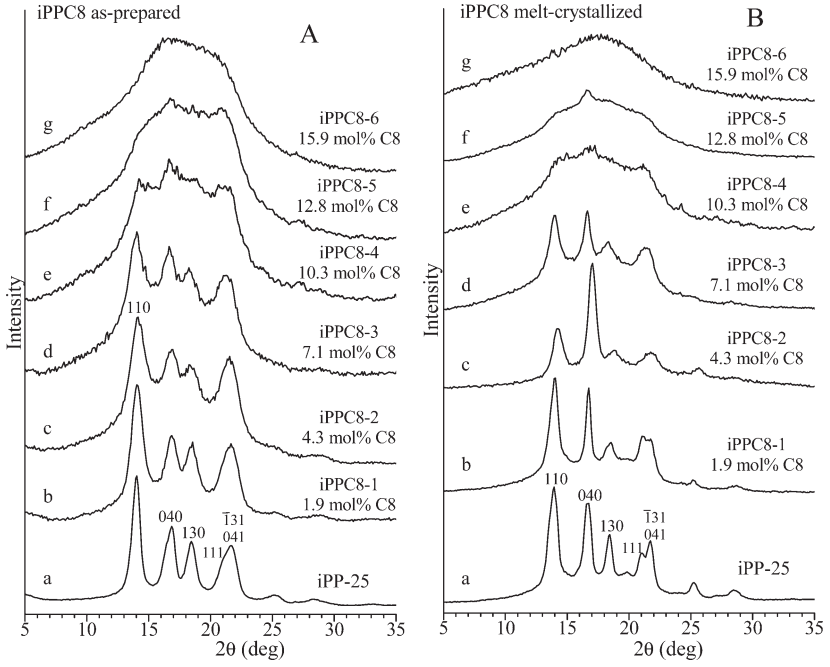

Figure 1. X-ray powder diffraction profiles of as-prepared (A) and melt-crystallized compression-molded samples (B) of iPPC8 copolymers of the indicated 1-octene concentration. The diffraction profiles of iPP homopolymer sample (iPP-25) prepared with the same catalyst (profiles a) are also reported. The 110, 040, 130, and (111 + $\bar{1}$31 + 041) reflections at $2\theta \approx 14°$, 17°, 18.6°, and 21−22°, respectively, of α form of iPP are indicated.

Figures 1 and 2, respectively. The melt-crystallized samples have been obtained by compression-molding and cooling to room temperature at cooling rate of 10 °C/min. The DSC melting curves of as-prepared samples of iPPC8 and iPPC18 copolymers are reported in Figure 3. The melting temperatures decrease with increasing comonomer concentration, and iPPC18 copolymers show melting temperatures lower than those of iPPC8 samples.

It is apparent that both as-prepared and melt-crystallized samples of iPP homopolymer and iPPC8 copolymers are crystallized only in the α form, up to octene concentration of nearly 10 mol %, as indicated by the presence of 110, 040, 130, and (111 + $\bar{1}$31 + 041) reflections at $2\theta \approx 14°$, 17°, 18.6°, and 21−22°, respectively, of α form of iPP and the absence of the 117 reflection of γ form at $2\theta = 20.1°$ in the diffraction profiles a−e of Figure 1A,B. For octene concentrations higher than 15−16 mol % the diffraction profiles show only a diffuse scattering, indicating that for these compositions iPPC8 copolymers are basically amorphous and are not able to crystallize in both as-prepared samples (profile g of Figure 1A) and samples cooled from the melt at 10 °C/min (profile g of Figure 1B). However, very small and broad reflections are still observed at $2\theta \approx 14°$, 17°, and 21° in the diffraction profile of the as-prepared sample iPPC8-5 with 12.8 mol % of octene (profile f of Figure 1A), whereas the amorphous scattering of the sample iPPC8-6 with 15.9 mol % of octene is clearly asymmetric with a broad peak at $2\theta = 14°$ (profile g of Figure 1A). This indicates that in these samples a very small level of crystallinity is still present. This is confirmed by the DSC melting curves of Figure 3A which show the presence of small melting peaks at 47 and 45 °C in the curves of the samples iPPC8-5 and iPPC8-6, respectively. Moreover, in the sample iPPC8-5 a small amount of defective α form crystallizes from the melt, as indicated by the presence of the small peak at $2\theta = 17°$ in the diffraction profile f of Figure 1B.

These data indicate that the presence of octene comonomeric units even at high concentrations induces neither the crystallization of the γ form, as occurs in copolymers of iPP with ethylene,[26] butene,[26] and hexene,[29] nor the crystallization of the trigonal form, as in the case of propylene−pentene[28] and propylene−hexene[24,25,29] copolymers.

In the case of iPPC18 copolymers, as-prepared samples having low octadecene content, up to nearly 1−2 mol %, are crystallized

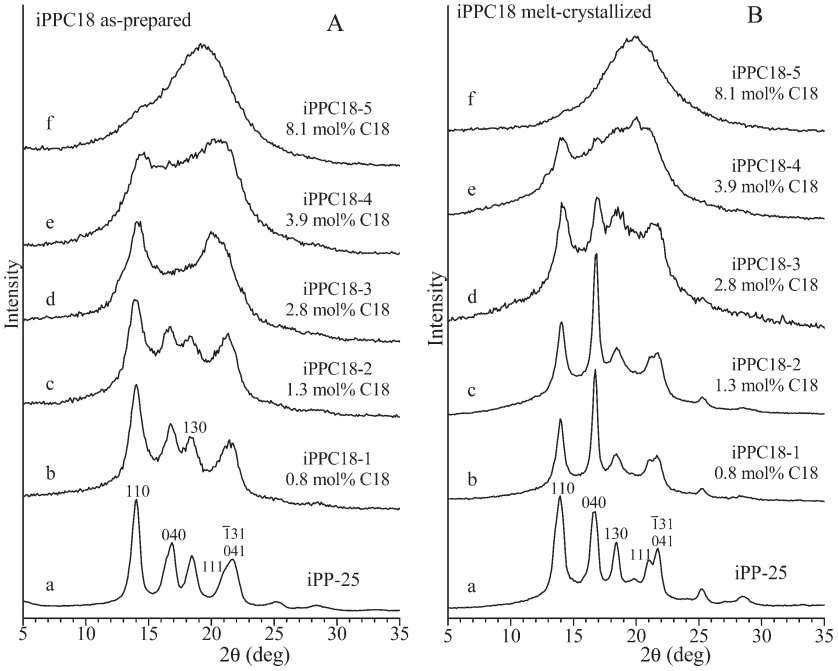

Figure 2. X-ray powder diffraction profiles of as-prepared (A) and melt-crystallized compression-molded samples (B) of iPPC18 copolymers of the indicated 1-octadecene concentration. The diffraction profiles of iPP homopolymer sample (iPP-25) prepared with the same catalyst (profiles a) are also reported. The 110, 040, 130, and (111 + $\bar{1}$31 + 041) reflections at $2\theta \approx 14°$, 17°, 18.6°, and 21−22°, respectively, of α form of iPP are indicated.

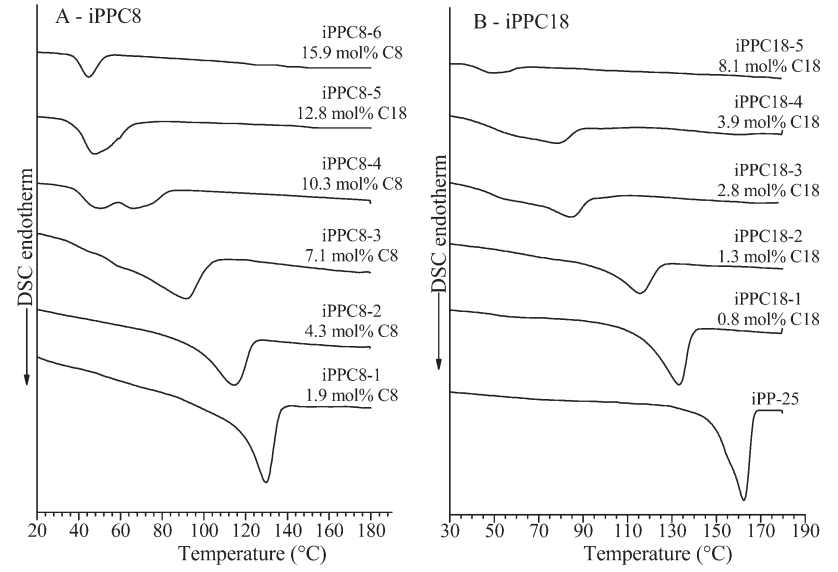

Figure 3. DSC heating curves of as-prepared samples of iPPC8 (A) and iPPC18 (B) copolymers recorded at heating rate of 10 °C/min. The melting curve of the as-prepared sample of the homopolymer iPP-25 is shown in (B).

in the α form, as shown by the diffraction profiles b and c of Figure 2A which present only the 110, 040, 130, and (111 + $\bar{1}$31 + 041) reflections at $2\theta \approx 14°$, 17°, 18.6°, and 21−22°, respectively, of the α form. The common crystallization of α form is no longer observed in as-prepared samples for octadecene concentrations higher than about 2 mol %. In fact, the diffraction profiles of the as-prepared samples of iPPC18 copolymers with 2.8 and 3.9 mol % of octadecene (profiles d and e of Figure 2A) do not present the 110, 040, 130, and (111 + $\bar{1}$31 + 041) reflections of the α form but show only two broad peaks at $2\theta = 14°$ and 20°. These data indicate that the iPPC18 copolymers with 2.8 and 3.9 mol % of octadecene crystallize probably in a highly disordered crystalline form different from the crystalline α and γ forms. Similar data have been reported in ref 21 and have been interpreted as a transformation at high comonomer concentration of the α form into the mesomorphic form of iPP,[21] along with a remarkable decrease of crystallinity. Moreover, the crystallite morphology changes from almost perfect spherulites to bundlelike crystals.[21]

For further increase of octadecene concentration (higher than 8 mol %), as-prepared samples of iPPC18 copolymers are basically amorphous (profile f of Figure 2A). It is worth remarking that the amorphous scattering halo of the sample iPPC18-5 with 8.1 mol % of octadecene presents a peak at $2\theta \approx 20°$, different from the amorphous halo of iPP, which shows a peak at $2\theta = 15°$. However, the DSC heating curves of samples iPPC18 of Figure 3B show that a small melting peak at 49 °C is still present in the melting curve of the sample iPPC18-5 with 8.1 mol % of octadecene, indicating that in this sample a very small level of crystallinity is still present.

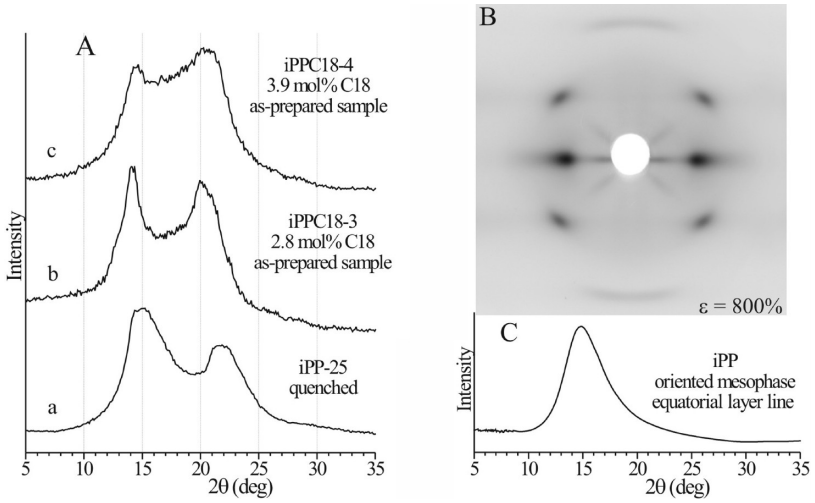

Figure 4. (A) X-ray powder diffraction profiles of the mesomorphic form of iPP, obtained from the sample of the homopolymer iPP-25 by quenching the melt to 0 °C (a) and of the as-prepared samples of the copolymers iPPC18-3 with 2.8 mol % of octadecene (b) and iPPC18-4 with 3.9 mol % of octadecene (c). (B, C) X-ray fiber diffraction pattern (B) and corresponding diffraction profile read along the equator (C) of fiber of iPP in the mesomorphic form, obtained by stretching at 800% deformation a sample of iPP homopolymer containing 5.9 mol % of *rr* stereo defects, crystallized initially in the γ form.[36a]

All samples of iPPC18 copolymers with octadecene concentration up to nearly 4−5 mol % and lower than 8 mol %, crystallize from the melt still in the α form (profiles b−e of Figure 2B). In particular, the sample iPPC18-3 with 2.8 mol % of octadecene, which is initially crystallized in a disordered mesomorphic modification (profile d of Figure 2A), crystallizes from the melt in the α form (profile d of Figure 2B). Samples with octadecene contents higher than 8 mol % are amorphous and do not crystallize from the melt by cooling the melt to room temperature at 10 °C/min (profile f of Figure 2B).

These data indicate that, as in the case of copolymers with 1-octene, the presence of 1-octadecene comonomeric units even at high concentrations does not induce the crystallization of the γ form but produces the formation in the as-prepared samples, rapidly crystallized from the polymerization medium, of a disordered mesomorphic form. From the data of Figure 1, it seems that this disordered mesomorphic form does not crystallize in as-prepared or melt-crystallized samples of iPPC8 copolymers. However, since the diffraction profiles of the as-prepared samples iPPC8-5 and iPPC8-6 with 12.8 and 15.9 mol % of octene, respectively, show a very small and broad diffraction peak at $2\theta \approx 14°$ (profiles f and g of Figure 1A), and the corresponding DSC curves present small melting peaks at 47 and 45 °C, respectively, the presence in these samples of crystals of the disordered mesomorphic form, also in mixture with defective crystals of α form, cannot be excluded.

Inspection of the X-ray diffraction profiles of Figure 1 and 2 also indicate that the 2θ positions of the 110 and 040 reflections of α form in the samples of iPPC8 and iPPC18 copolymers are basically the same as those in the diffraction profile of the iPP homopolymer sample, in both as-prepared (Figures 1A and 2A) and melt-crystallized (Figures 1B and 2B) samples. This indicates that 1-octene and 1-octadecene comonomeric units are excluded from the crystals of α form of iPP. We recall that in the case of copolymers of iPP with butene,[26] pentene,[28] and hexene[24,25,29] the comonomers are included in the crystals of α form of iPP, as demonstrated by the increase of the unit cell parameters with the comonomer concentration, and induce crystallization of the α form and, for pentene and hexene at high concentrations, of the trigonal form of iPP.

As mentioned above, the formation of the mesomorphic form of iPP in iPPC18 copolymers when the octadecene concentration achieves 2−3 mol % was suggested in ref 21 on the basis of the X-ray diffraction profiles similar to that of profile d of Figure 2A, which present only two broad peaks at $2\theta = 14°$ and 20°. This diffraction profile is, indeed, similar to the diffraction profiles of the well-known solid mesophase of iPP that is generally obtained in iPP homopolymer samples by quenching the melt to low temperatures (nearly 0 °C).[43] A comparison between the X-ray powder diffraction profiles of the mesophase of iPP, obtained by quenching the melt of the homopolymer sample iPP-25 to 0 °C, and the X-ray powder diffraction profiles of the as-prepared samples of the copolymers iPPC18-3 and iPPC18-4 with 2.8 and 3.9 mol % of octadecene (profiles d and e of Figure 1A) are reported in Figure 4A. The X-ray fiber diffraction pattern of the mesophase of iPP, taken from the literature,[36a] obtained by stretching at high deformations a sample of iPP homopolymer containing 5.9 mol % of *rr* stereodefects, crystallized initially in the γ form,[36a] is reported in Figure 4B. It is worth noting that similar fibers of the mesomorphic form of iPP and similar fiber diffraction patterns have been obtained by stretching at high deformations films of iPP homopolymer in the quenched mesomorphic form.[44] From the powder diffraction profile (profile a of Figure 4A) and the fiber pattern (Figure 4B) the most important structural features of the mesomorphic form of iPP have been clarified.[38,44,45] The two broad reflections observed in the powder diffraction profile at $2\theta = 15°$ ($d = 5.88$ Å) and 21.3° ($d = 4.17$ Å) (profile a of Figure 4A) are in the fiber diffraction pattern confined along different layer lines (Figure 4B). The reflection at $2\theta = 15°$ is an equatorial reflection ($l = 0$), whereas the reflection peak at $2\theta = 21.3°$ corresponds to a first layer line reflection (Figure 4B).[38,44] The layering of the diffracted intensity in the fiber pattern of the mesophase and the corresponding measured values of the chain axis c of 6.5 Å[44] have indicated that the mesophase of iPP is composed of bundles of parallel chains in the ordered 3-fold helical conformation.[38,43,44] The order of the atomic positions (and hence the correlation of interatomic distances) in the direction of the chain axes spans a range longer than in the perpendicular directions. The lateral order is, indeed, not so well developed as conformational order, though the relative heights of the neighboring chains within each bundle are mainly correlated. The local correlations between chains inside each small mesomorphic aggregate are similar to those characterizing the crystal structure of the monoclinic α form,[38,45] that is, the facing of enantiomorphous 3/1 helical chains. In these bundles of chains any correlation about the relative position of the atoms is lost at distances of the order of 40−50 Å.[38]

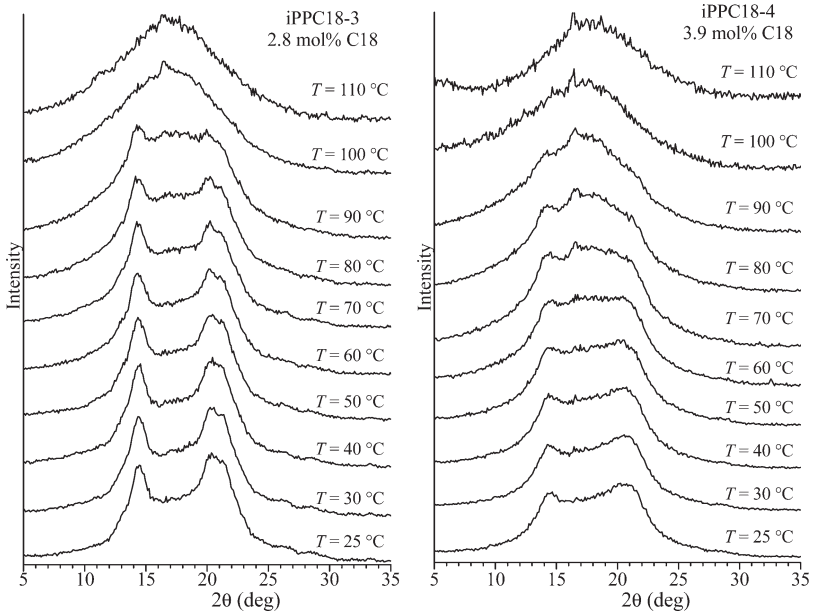

Figure 5. X-ray powder diffraction profiles of the as-prepared samples of the copolymers iPPC18-3 with 2.8 mol % of octadecene (A) and iPPC18-4 with 3.9 mol % of octadecene (B) recorded at different increasing temperatures up to the melt.

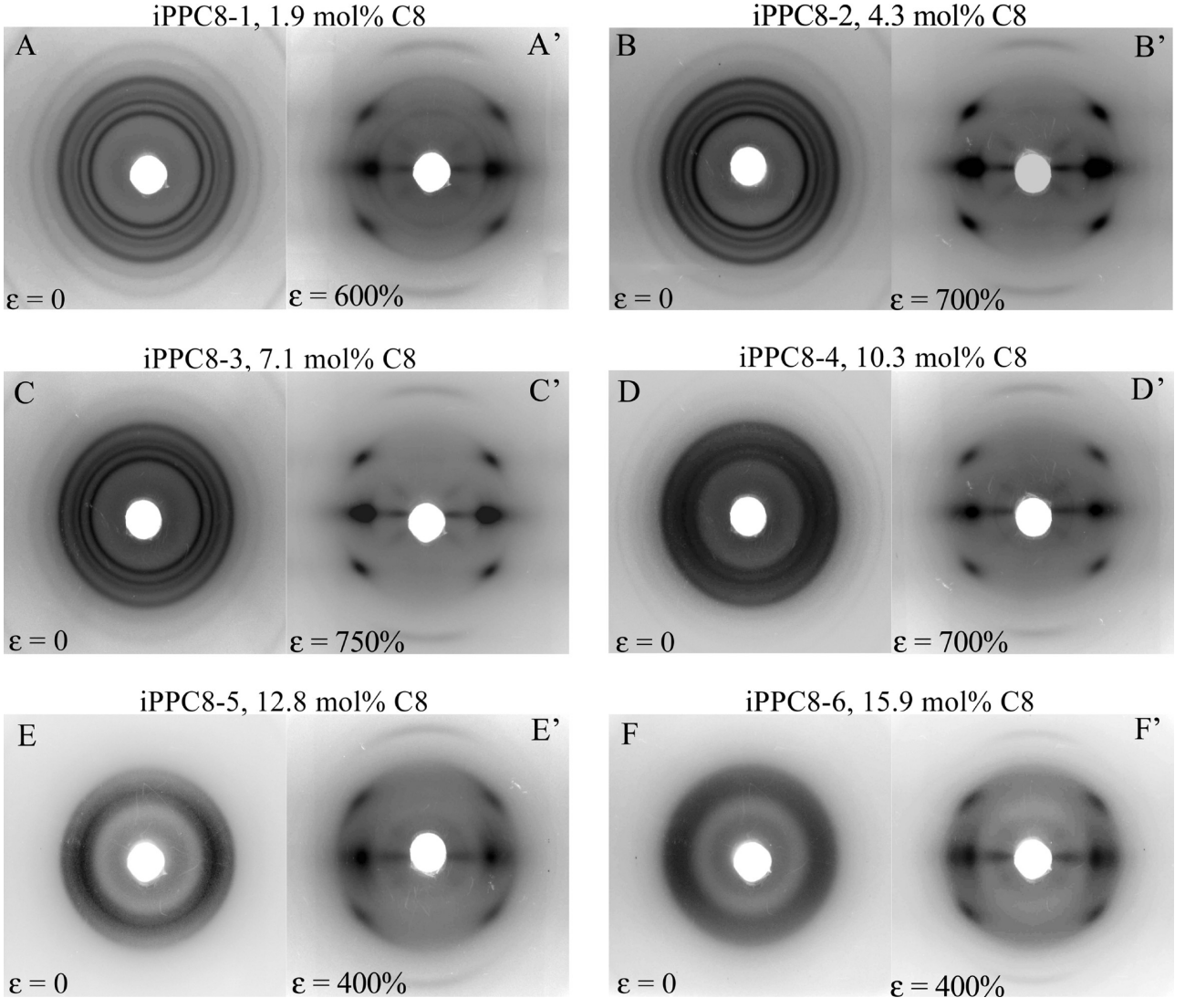

Figure 6. X-ray diffraction patterns of fibers of iPPC8 copolymers, unstretched (A−F) and stretched up the maximum possible deformation ε (A′−F′).

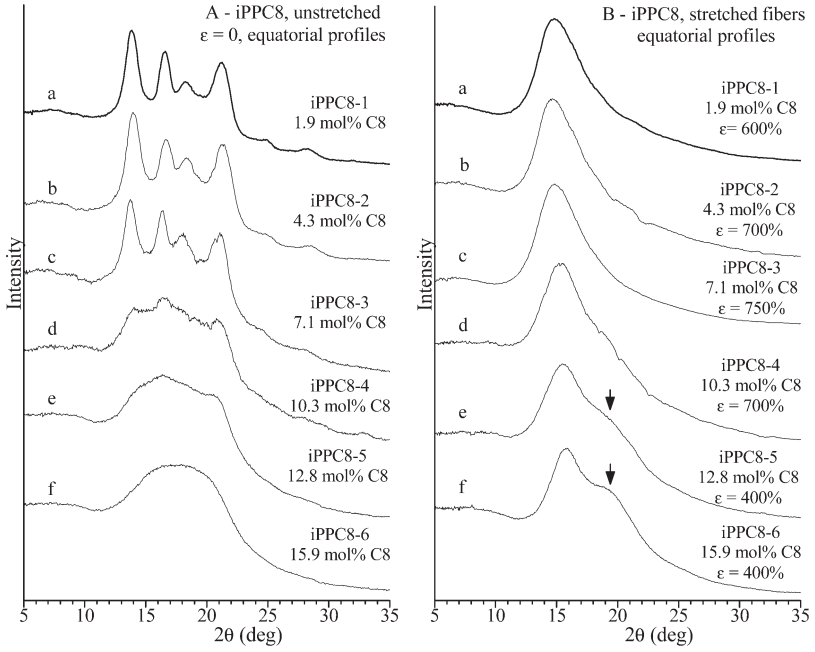

Figure 7. X-ray diffraction profiles read along the equator of the fiber diffraction patterns of Figure 6 of iPPC8 copolymers: unstretched films (A) and stretched up the maximum possible deformation ε (B). The arrows indicate the reflection that is present on the equator of the diffraction patterns of the new mesomorphic form and absent in the diffraction patterns of the classic mesophase of iPP.

The comparison of Figure 4 indicates that the ratio between the intensities of the two broad peaks at $2\theta = 15°$ and 21.3° in the powder pattern of the mesophase of iPP (profile a of Figure 4A) is much higher than the ratio between the intensities of the two broad peaks observed at $2\theta = 14°$ and 20° in the diffraction profiles of the mesomorphic form crystallized in the copolymers iPPC18-3 and iPPC18-4 with 2.8 and 3.9 mol % of octadecene (profiles b and c of Figure 4A). Moreover, the 2θ positions of the peaks in the diffraction profiles of the mesophase in the copolymer samples ($2\theta = 14°$ and 20°) are different from the positions of the peaks in the diffraction profile of the mesophase of iPP ($2\theta = 15°$ and 21.3°). These observations suggest that the mesomorphic form that crystallize in the iPPC18 copolymers is different from the well-known quenched mesophase of the iPP homopolymer.

A further difference between the mesophase of iPPC18 copolymers and the quenched mesophase of iPP can be evidenced through thermal treatments experiments. It is well-known that the quenched mesophase of iPP transforms into the stable α form by annealing in the temperature range 50−80 °C.[43] The X-ray powder diffraction profiles of the as-prepared samples of iPPC18-3 and iPPC18-4 copolymers with 2.8 and 3.9 mol % of octadecene recorded at different increasing values of temperature are shown in Figure 5. It is apparent that both samples do not transform into α form by thermal treatments and then melt at temperatures higher than 90 °C. Only a small reflection at $2\theta = 17°$ appears at 90−100 °C for the sample iPPC18-3 (Figure 5A) and at 70−80 °C for the sample iPPC18-4 (Figure 5B), indicating that a small amount of crystals of α form develops at high temperatures.

Details of the structural differences between the solid mesophases of iPP and of iPPC18 copolymers can be clarified through analysis of the diffraction patterns of oriented fibers of iPPC8 and iPPC18 copolymers. Compression-molded films of iPPC8 and iPPC18 copolymers, which are crystallized in the α form for low comonomer concentrations and are amorphous for high comonomer concentrations (Figures 1B and 2B), have been stretched at room temperature, and the X-ray fiber diffraction patterns have been recorded.

The bidimensional X-ray diffraction patterns of compression-molded films of the iPPC8 copolymers before stretching (deformation $\varepsilon = 0$) and the fiber diffraction patterns of the same film stretched up to the maximum possible deformation ε are reported in Figure 6. For each pattern, the corresponding diffraction profiles read along the equatorial layer lines are reported in Figure 7. As discussed above (Figure 1B), melt-crystallized compression-molded films of iPPC8 copolymers with low octene concentration, up to nearly 10 mol %, are crystallized in the α form, as indicated by the presence of 110, 040, and 130 reflections at $2\theta \approx 14°$, 17°, and 18.6° of α form of iPP in the patterns of Figure 6A−D and in the equatorial profiles a−d of Figure 7A. In these samples crystals of α form, present in the compression-molded films, transform by stretching into the mesomorphic form of iPP, as indicated by the transformation of the three equatorial reflections 110, 040, and 130 of α form into the broad halo in the range $2\theta = 14−16°$, centered at $2\theta = 15°$ (patterns A′−D′ of Figure 6 and equatorial profiles a−d of Figure 7B). Also in the case of the nearly amorphous sample iPPC8-4 with 10.3 mol % octene (pattern D of Figure 6 and profile d of Figure 7A), the stretching produces crystallization of the mesomorphic form (patterns D′ of Figure 6 and d of Figure 7B). At high degrees of deformation well-oriented fibers of the pure mesomorphic form are obtained for the iPPC8 samples having octene concentrations lower than 12 mol % (patterns A′−D′ of Figure 6 and profiles a−d of Figure 7B). It is worth noting that the mesomorphic phase obtained in these samples of iPPC8 copolymer corresponds to the mesomorphic form of iPP of Figure 4B. In fact, the equatorial diffraction profiles a−d of Figure 7B present only one broad peak at $2\theta = 15°$, as in the mesophase of iPP (Figure 4B,C). The second broad peak at $2\theta = 21.3°$ of the mesophase is present on the first layer line of the patterns A′−D′ of Figure 6 and is, therefore, absent on the equatorial profiles of Figure 7B. In other words, whereas the powder diffraction profile of the mesophase of iPP show two broad peaks at $2\theta = 15°$ and 21.3° (profile a of Figure 4A), the equatorial profile of the X-ray fiber diffraction pattern of a fiber of the mesophase must present only the equatorial reflection at $2\theta = 15°$, as in Figure 4C.

The compression-molded films of iPPC8 copolymers with octene concentrations higher than 12 mol % are basically amorphous (patterns E, F of Figure 6 and profiles e, f of Figure 7A). As discussed above, in the sample iPPC8-5 a small amount of defective α form crystallize from the melt, as indicated by the presence of the small peak at $2\theta = 17°$ in the diffraction pattern of Figure 6E (profiles f of Figure 1B and e of Figure 7A). The stretching at high deformation of these samples produces crystallization of a well-oriented mesomorphic form, as indicated by the transformation of the broad amorphous haloes in the patterns E, F of Figure 6 into less broad diffraction peaks, which are present on the equator and on the first layer line of the patterns E′, F′ of Figure 6. In particular, on the equatorial diffraction profiles e, f of Figure 7B, besides the diffraction peak centered at $2\theta = 15°$, a new second diffraction peak at $2\theta \approx 20°$ appears. This peak is not present in the X-ray fiber diffraction patterns of the mesomorphic form of iPP of Figure 4B,C.

These data indicate that the solid mesophase that forms by stretching of iPPC8 copolymers with high octene concentration is different from the mesomorphic form of iPP. This second equatorial diffraction peak at $2\theta \approx 20°$ is present in the fiber diffraction patterns E′, F′ of Figure 6 and e, f of Figure 7B only as a shoulder of the peak at $2\theta = 15°$ and becomes much more evident in the X-ray diffraction patterns of oriented fibers of iPPC18 copolymers. This peak, indeed, recalls the reflection observed at $2\theta = 20°$ in the X-ray powder diffraction profiles of the as-prepared samples of iPPC18 copolymers with 2.8 and 3.4 mol % of octadecene of Figure 2A (profiles d, e of Figure 2A and Figure 5).

The bidimensional X-ray diffraction patterns of compression-molded films of the iPPC18 copolymers before stretching ($\varepsilon = 0$) and the fiber diffraction patterns of the same films stretched up to the maximum possible deformation ε are reported in Figure 8. For each pattern, the corresponding diffraction profiles read along the equatorial layer lines are reported in Figure 9. As also shown in Figure 2B, compression-molded films of iPPC18 copolymers with low octadecene concentration, up to 2.8 mol %, are crystallized in the α form of iPP (patterns A−C of Figure 8 and profiles a−c of Figure 9A), whereas the sample iPPC18-4 with 3.9 mol % of octadecene is crystallized in the mesomorphic form, as indicated by the presence of the two broad peaks at $2\theta = 14°$ and 20° (pattern D of Figure 8 and profile d of Figure 9A). In the samples iPPC18-1 and iPPC18-2 with very low octadecene concentrations (0.8 and 1.3 mol %, respectively), crystals of α form, present in the compression-molded films, transform by stretching into the mesomorphic form of iPP, as indicated by the transformation of the three equatorial reflections 110, 040, and 130 of α form into the broad halo in the range $2\theta = 14-16°$, centered at $2\theta = 15°$ (patterns A′, B′ of Figure 8 and equatorial profiles a, b of Figure 9B) and the presence of a single peak at $2\theta = 15°$ on the equator, even though with a small shoulder at $2\theta = 19-20°$.

The stretching of the sample iPPC18-3 with 2.8 mol % of octadecene that is still crystallized in the α form (pattern C of Figure 8 and profile c of Figure 9A) produces transformation of the three equatorial reflections 110, 040, and 130 of α form into a broad peak centered at $2\theta = 14°$, while a well-defined second peak appears on the equator at $2\theta \approx 20°$ (pattern C′ of Figure 8 and profile c of Figure 9B), along with the usual first layer line reflection at $2\theta \approx 20-21°$ (pattern C′ of Figure 8). The equatorial reflection at $2\theta = 20°$ is not present in the X-ray fiber diffraction patterns of the mesomorphic form of iPP of Figure 4B,C. These data indicate that for this iPPC18 sample crystals of α form of iPP transforms by stretching into a mesophase different from the mesomorphic form of iPP. The fiber diffraction pattern of the new mesophase (patterns C′ of Figure 8 and c of Figure 9B)

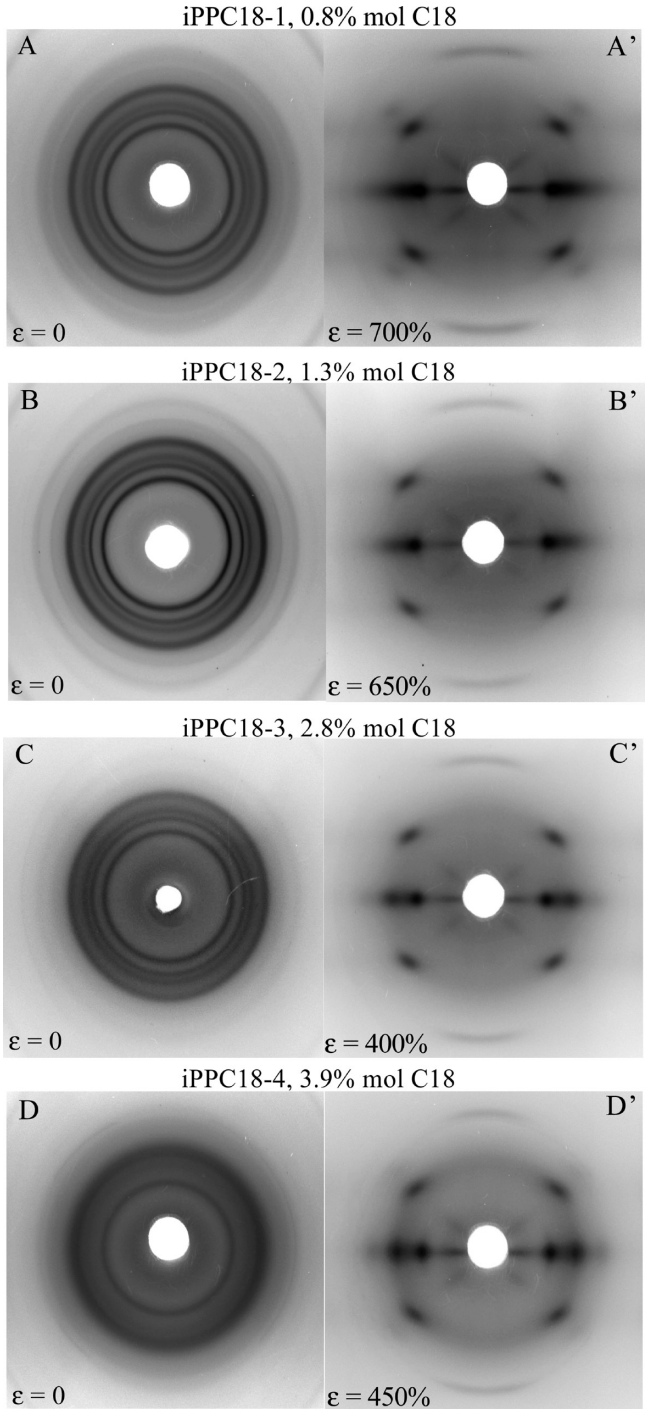

Figure 8. X-ray diffraction patterns of fibers of iPPC18 copolymers: unstretched (A−D) and stretched up the maximum possible deformation ε (A′−D′).

presents the same reflections at $2\theta = 14°$ and 20° observed in the X-ray powder diffraction profile of the as-prepared specimen of the same sample iPPC18-3 with 2.8 mol % of octadecene (profile d of Figure 2A). This indicates the iPPC18-3 copolymer sample crystallizes in the new mesomorphic form in the as-prepared sample (profile d of Figure 2A), then crystallizes in the α form of iPP by melt-crystallization (profile d of Figure 2B, pattern C of Figure 8, and profile c of Figure 9A), and, finally, the α form transforms again into the new mesophase by stretching (Figure 8C′ and profile c of Figure 9B).

Melt-crystallized compression-molded films of the sample iPPC18-4 with 3.9 mol % of octadecene are crystallized in the

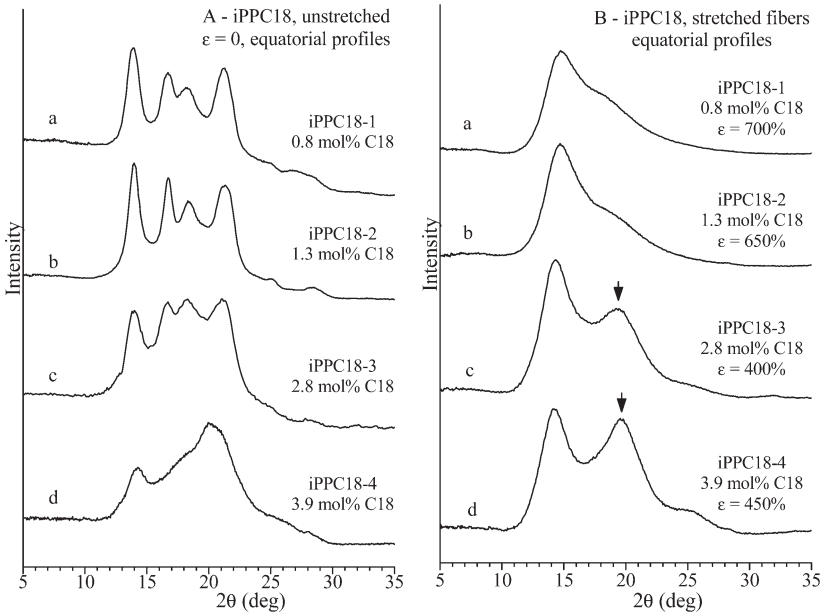

Figure 9. X-ray diffraction profiles read along the equator of the fiber diffraction patterns of Figure 8 of iPPC18 copolymers: unstretched films (A) and stretched up the maximum possible deformation ε (B). The arrows indicate the reflection that is present on the equator of the diffraction patterns of the new mesomorphic form and absent in the diffraction patterns of the classic mesophase of iPP.

new mesomorphic form (pattern D of Figure 8 and profile d of Figure 9A) (as in the as-prepared sample). The stretching of this sample produces orientation of the mesophase and well-oriented fibers of the new mesophase are obtained, and the two broad peaks at $2\theta = 14°$ and 20° become polarized on the equator (pattern D′ of Figure 8 and profile d′ of Figure 9B). This confirms that the peak at $2\theta = 20°$ in the powder diffraction profiles of the mesophase that crystallize in the as-prepared samples of the copolymers iPPC18-3 and iPPC18-4 with 2.8 and 3.9 mol % of octadecene (profiles d, e of Figure 2A) and in the melt-crystallized sample of the copolymer iPPC18-4 (profile e of Figure 2B) is an equatorial reflection. Hence, this disordered modification that crystallize in fibers of iPPC8 copolymers and in powder samples and fibers of iPPC18 copolymers is a new mesophase different from the mesomorphic form of iPP.

Samples of iPPC18 copolymers with octadecene concentration higher than 7−8 mol % are amorphous and do not crystallize by stretching.

From the X-ray fiber diffraction patterns of the new mesophase of iPPC8 and iPPC18 copolymers, in particular from the diffraction pattern of the well-developed mesophase of the samples iPPC18-3 and iPPC18-4 with 2.8 and 3.9 mol % of octadecene of Figures 8C′ and 8D′, respectively, a value of the chain axis of the new mesophase of 6.5−6.6 Å has been determined. This indicates that the chains of the new mesophase are in the ordered 3/1 helical conformation, as for the classic mesophase of the iPP homopolymer.[43]

As discussed above, we recall that the mesomorphic form of iPP may be obtained by rapid quenching the melt to low temperatures and by transformation of the α or γ forms by stretching. The stress-induced transformation of α form into the mesophase has been observed in iPP homopolymer samples prepared with Ziegler−Natta[37,39] as well as metallocene catalysts[35,36] and in copolymers of iPP with butene and hexene.[27,30] It has been suggested that this transformation occurs through the destruction of the lamellar crystalline phase, probably by pulling chains out from crystals and successive reorganization of the chains in the crystalline mesomorphic aggregates.[37] In the case of iPPC18 copolymers the new mesomorphic form is also obtained by stretching crystals of α form (Figure 8C,C′), whereas in the case of iPPC8 copolymers it is obtained by stress-induced crystallization of amorphous samples (Figure 6F,F′). We can assume that the formation of the mesomorphic form may occur not only via the pulling out of the chains from the lamellae of pre-existing crystalline form and successive reorganization of the chains in the crystalline mesomorphic aggregates, but also by direct crystallization of the amorphous chains in the case of iPPC8 copolymers. Moreover, for longer branched iPPC18 copolymers with octadecene concentration in the range 2−4 mol %, the new mesophase can also be obtained in as-prepared and melt-crystallized samples without quenching. It is worth recalling that in the case of other copolymers of iPP with less branched comonomers, like butene and hexene, the mesomorphic form of iPP has been obtained by stretching, but it has never been observed in as-prepared or melt-crystallized samples of the copolymers.[27,30] As for the iPP homopolymer, for these copolymers the mesophase can be obtained by quenching the melt.[23,39]

The data of Figures 6−9 indicate that, whereas in unoriented powder as-prepared or melt-crystallized samples there is a clear difference between samples that crystallize in the α form of iPP (at low comonomer concentrations) and samples that crystallize in the new mesophase (at higher comonomer concentration), in fiber specimens there is a nearly continuous variation of structural organization from the mesophase found in pure iPP to the new mesophase of the fibers of the sample iPPC18-4, as suggested by the continuous increase of the intensity of the equatorial reflection at $2\theta = 20°$ (Figures 7B and 9B).

These observations suggest that the easy formation of the mesomorphic form in highly branched iPP copolymers and the corresponding structure are related to the presence of the long flexible side groups. This behavior seems similar to the comblike polymers, as poly(di-*n*-alkylsiloxanes) and poly(phosphazenes) which show pseudohexagonal mesophases characterized by a high degree of conformational disorder not only of the polymer backbone but also of the flexible side groups.[46−48] According to a generalized view given by Allegra and Meille,[48] these mesophases gain entropy from optimization of the organization of the side groups and the chain backbone; the flexible main chains, indeed, become quite rigid as a consequence of their "self-compacting" elastic nature, due to the presence of lateral groups.[48] In the case

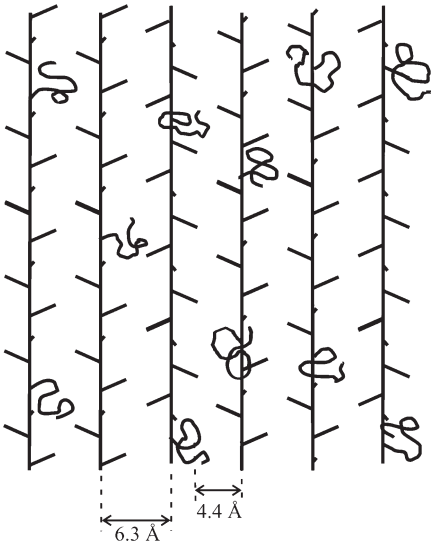

Figure 10. Schematic model of the organization of chains of iPPC18 copolymers in the new mesophase. The mesomorphic aggregates are characterized by parallel chains in the ordered 3/1 helical conformation with periodicity of nearly 6.5 Å packed at average interchain distances of about 6.3 Å, defined by the self-organization of the flexible disordered side groups with average distance between branches or between main chains and branches of about 4.4 Å.

of iPPC18 copolymers, the long flexible C_{16} side groups do not disturb the 3/1 helix of the main chain and make the chain backbone quite rigid, favoring the organization of the 3/1 helical chains in the mesomorphic aggregates.

The structure of these mesomorphic aggregates is different from that of the quenched solid mesophase of the iPP homopolymer.[38] In fact, the dominant constituent of the mesomorphic aggregates of iPP are bundles of chains in the ordered 3-fold helical conformation, which are locally packed at very short-range distances as in the crystals of α form.[38,45] These local lateral correlations are rapidly lost at distances higher than 40−50 Å, so that the mesomorphic aggregates are mainly characterized by conformational order and high degree of disorder in the lateral packing of chains.[38]

In the case of the new mesophase of iPPC18 copolymers, the presence of the equatorial reflections of strong intensity at 2θ = 14° and 20° (d = 6.33 and 4.44 Å, respectively), of other two low-intensity equatorial reflections at 2θ = 25.2° and 28.4° (d = 3.6 and 3.1 Å, respectively) (Figure 8D′ and profile d of Figure 9B) and of the first layer line reflection at $2\theta \approx 20°$, indicates that the structure of the mesomorphic aggregates is characterized by parallel chains in 3/1 helical conformation packed at average interchain distances of about 6 Å, defined by the self-organization of the flexible side groups, which, in turn, produces the equatorial reflection at 2θ = 20° (d = 4.44 Å). This reflection is, indeed, at nearly the same 2θ position as that of the maximum of the diffuse halo observed in the X-ray diffraction profiles of amorphous iPPC18 copolymer samples having octadecene content higher than 7−8 mol % (profile f of Figure 2A,B) and probably reflects the average distance of about 4.4 Å between the disordered branches or between the main chains and branches. Moreover, the presence of the small equatorial reflections at 2θ = 25.2° and 28.4° indicates that some lateral short-range correlation between the chains is maintained. We have determined by flotation the values of the experimental densities of the samples iPPC18-3 and iPPC18-4 with 2.8 and 3.9 mol % of octadecene, which crystallize in the new mesophase (Figures 2d,e and 5). The values of 0.887 g/cm^3 for the sample iPPC18-3 and 0.877 g/cm^3 for the sample iPPC18-4 have been found, which correspond in both cases to a density of the crystalline mesomorphic phase of nearly 0.9 g/cm^3, for degrees of crystallinity of nearly 50−55%, and assuming the value of 0.854 g/cm^3 for the density of the amorphous phase.[49] The relatively high value of the crystalline density, higher than the density of the amorphous iPP, indicates a dense, although disordered, crystalline mesomorphic phase, according to the presence of the short-range order in the lateral packing of parallel 3/1 helices.

It is worth remarking that the characteristic equatorial reflection at d = 6.33 and 4.44 Å of the new mesophase, which develop in our long branched iPP copolymers, do not correspond to the typical 100 and 110 reflections of a pseudohexagonal structure that is generally observed in many solid mesophases, as, for instance, in long branched poly(di-*n*-alkylsiloxanes) and poly(phosphazenes).[48] They rather reflect the average interchain distance and the average distance between branches or between main chains and branches, respectively. Therefore, at variance with the pseudohexagonal mesophases characterized by long-range order in the lateral packing of the chain axes and disorder along directions parallel to the chain axes,[46−48] due to the disorder in the conformation of the chains and the absence of any lateral correlations between atoms, in the new mesophase of long branched iPP copolymers there is short-range order in the lateral packing of the chain axes and long-range order is maintained only in the regular conformation of the 3/1 helices with periodicity of nearly 6.5 Å. The random placements of comonomers with long side groups along the chains and the high degree of stereoregularity of the isotactic copolymers, achieved resorting to metallorganic catalytic systems, allow maintaining the regular 3/1 helical conformation over long portions of the copolymer chains. The presence of the long branches prevents crystallization of the normal α and γ forms of iPP and induces formation of the mesomorphic aggregates with absence of any lateral order. The parallel arrangement of defective portions of chains in 3/1 helical conformation in the mesomorphic domains not only maximize the entropy from optimization of the organization of the side groups and the chain backbone but also produces a neat increase in enthalpy.[48] The long alkyl side groups, indeed, have low affinity with the chain backbone and prefer to maximize their interaction facing each other as sketched in the model of Figure 10.

Conclusions

Isotactic propylene−1-octene and propylene−1-octadecene copolymers have been synthesized with a highly isospecific C_2-symmetric metallocene catalyst. The crystallization properties of the copolymers in as-prepared and melt-crystallized samples and in oriented fibers have been analyzed as a function of the comonomer concentration. iPPC8 copolymers crystallize in the α form of iPP for octene concentration up to 12−13 mol %, whereas iPPC18 copolymers crystallize in the α form for very low octadecene concentration and in a new mesomorphic form for octadecene contents higher than 2−3 mol %. In both copolymers crystals of α form transform into the new mesophase by stretching at high deformations.

The powder diffraction profile and the fiber diffraction pattern of the mesophase have indicated that the mesomophic form that crystallize in these long branched copolymers is different from the classic mesophase of the iPP homopolymer that is, generally, obtained by quenching the melt to low temperatures. In fact, the diffraction patterns of the new mesophase of iPPC18 copolymers present a strong equatorial reflection at 2θ = 20°, which is absent in the diffraction pattern of the mesophase of iPP. Moreover, from the fiber diffraction pattern a value of the chain axis of 6.5−6.6 Å of the new mesophase has been evaluated, indicating that this mesophase is characterized by chains in the ordered 3/1

helical conformation, and high degree of disorder in the lateral packing of the chains.

The easy formation of the mesomorphic form in highly branched iPP copolymers and the corresponding structure are related to the presence of the long flexible side groups. In the iPPC18 copolymers, the long flexible C_{16} side groups do not disturb the 3/1 helix of the main chain and make the chain backbone quite rigid, favoring the organization of the 3/1 helical chains in the mesomorphic aggregates. These mesomorphic aggregates are characterized by parallel chains in 3/1 helical conformation packed at average interchain distances of about 6 Å, defined by the self-organization of the flexible side groups.

Acknowledgment. Financial support from Basell Polyolefins, Ferrara (Italy), is gratefully acknowledged. We thank G. Talarico for the synthesis of the copolymer samples.

References and Notes

(1) Arnold, M.; Henschke, O.; Knorr, J. *Macromol. Chem. Phys.* **1996**, *197*, 563.
(2) Arnold, M.; Bornemann, S.; Köller, F.; Menke, T. J.; Kressler, J. *Macromol. Chem. Phys.* **1998**, *199*, 2647.
(3) Busse, K.; Kressler, J.; Maier, R. D.; Scherble, J. *Macromolecules* **2000**, *33*, 8775.
(4) (a) Forlini, F.; Tritto, I.; Locatelli, P.; Sacchi, M. C.; Piemontesi, F. *Macromol. Chem. Phys.* **2000**, *201*, 401. (b) Costa, G.; Stagnaro, P.; Trefiletti, V.; Sacchi, M. C.; Forlini, F.; Alfonso, G. C.; Tincul, I.; Wahner, U. M. *Macromol. Chem. Phys.* **2004**, *205*, 383. (c) Stagnaro, P.; Costa, G.; Trefiletti, V.; Canetti, M.; Forlini, F.; Alfonso, G. C. *Macromol. Chem. Phys.* **2006**, *207*, 2128.
(5) (a) Kim, I. *Macromol. Rapid Commun.* **1998**, *19*, 299. (b) Kim, I.; Kim, Y. I. *Polym. Bull.* **1998**, *40*, 415.
(6) Alamo, R. G.; Isasi, J. R.; Kim, M.-H.; Mandelkern, L.; VanderHart, D. L. *Polym. Mater. Sci. Eng. Proc.* **1999**, *81*, 346.
(7) Alamo, R. G.; VanderHart, D. L.; Nyden, M. R.; Mandelkern, L. *Macromolecules* **2000**, *33*, 6094.
(8) Hosier, I. L.; Alamo, R. G.; Esteso, P.; Isasi, G. R.; Mandelkern, L. *Macromolecules* **2003**, *36*, 5623.
(9) Hosier, I. L.; Alamo, R. G.; Lin, J. S. *Polymer* **2004**, *45*, 3441.
(10) Alamo, R. G.; Ghosal, A.; Chatterjee, J.; Thompson, K. L. *Polymer* **2005**, *46*, 8774.
(11) Fan, Z.; Yasin, T.; Feng, L. *J. Polym. Sci., Part A* **2000**, *38*, 4299.
(12) (a) Van Reenen, A. J.; Brull, R.; Wahner, U. M.; Pasch, H. *Polym. Prepr.* **2000**, *41* (1), 496. (b) Brull, R.; Pasch, H.; Rauberheimer, H. G.; Sanderson, R. D.; Wahner, U. M. *J. Polym. Sci., Part A: Polym. Chem.* **2000**, *38*, 2333. (c) Van Reenen, A. J.; Brull, R.; Wahner, U. M.; Raubenheimer, H. G.; Sanderson, R. D.; Pasch, H. *J. Polym. Sci., Part A: Polym. Chem.* **2000**, *38*, 4110. (d) Brüll, R.; Pasch, H.; Raubenheimer, H. G.; Sanderson, R.; van Reenen, A. J.; Wahner, U. M. *Macromol. Chem. Phys.* **2001**, *202*, 1281.
(13) Lovisi, H.; Tavares, M. I. B.; da Silva, N. M.; de Menezes, S. M. C.; de Santa Maria, L. C.; Coutinho, F. M. B. *Polymer* **2001**, *42*, 9791.
(14) Shin, Y.-W.; Uozumi, T.; Terano, M.; Nitta, K.-H. *Polymer* **2001**, *42*, 9611.
(15) Shin, Y.-W.; Hashiguchi, H.; Terano, M.; Nitta, K. *J. Appl. Polym. Sci.* **2004**, *92*, 2949.
(16) Hosoda, S.; Hori, H.; Yada, K.; Tsuji, M.; Nakahara, S. *Polymer* **2002**, *43*, 7451.
(17) Fujiyama, M.; Inata, H. *J. Appl. Polym. Sci.* **2002**, *85*, 1851.
(18) Xu, J.-T.; Xue, L.; Fan, Z.-Q. *J. Appl. Polym. Sci.* **2004**, *93*, 1724.
(19) Poon, B.; Rogunova, M.; Chum, S. P.; Hiltner, A.; Baer, E. *J. Polym. Sci., Polym. Phys.* **2004**, *42*, 4357.
(20) Poon, B.; Rogunova, M.; Hiltner, A.; Baer, E.; Chum, S. P.; Galeski, A.; Piorkowska, E. *Macromolecules* **2005**, *38*, 1232.
(21) Palza, H.; López-Majada, J. M.; Quijada, R.; Benavente, R.; Pérez, E.; Cerrada, M. L. *Macromol. Chem. Phys.* **2005**, *206*, 1221.
(22) López-Majada, J. M.; Palza, H.; Guevara, J. L.; Quijada, R.; Martinez, M. C.; Benavente, R.; Pereña, J. M.; Pérez, E.; Cerrada, M. L. *J. Polym. Sci., Polym. Phys. Ed.* **2006**, *44*, 1253.
(23) Cerrada, M. L.; Polo-Corpa, M. J.; Benavente, R.; Pérez, E.; Velilla, T.; Quijada, R. *Macromolecules* **2009**, *42*, 702.
(24) De Rosa, C.; Auriemma, F.; Corradini, P.; Tarallo, O.; Dello Iacono, S.; Ciaccia, E.; Resconi, L. *J. Am. Chem. Soc.* **2006**, *128*, 80.
(25) De Rosa, C.; Dello Iacono, S.; Auriemma, F.; Ciaccia, E.; Resconi, L. *Macromolecules* **2006**, *39*, 6098.
(26) De Rosa, C.; Auriemma, F.; Ruiz de Ballesteros, O.; Resconi, L.; Camurati, I. *Macromolecules* **2007**, *40*, 6600.
(27) De Rosa, C.; Auriemma, F.; Ruiz de Ballesteros, O.; Resconi, L.; Camurati, I. *Chem. Mater.* **2007**, *19*, 5122.
(28) De Rosa, C.; Auriemma, F.; Talarico, G.; Ruiz de Ballesteros, O. *Macromolecules* **2007**, *40*, 8531.
(29) De Rosa, C.; Auriemma, F.; Ruiz de Ballesteros, O.; De Luca, D.; Resconi, L. *Macromolecules* **2008**, *41*, 2172.
(30) De Rosa, C.; Auriemma, F.; Ruiz de Ballesteros, O.; Dello Iacono, S.; De Luca, D.; Resconi, L. *Cryst. Growth Des.* **2009**, *9*, 165.
(31) Lotz, B.; Ruan, J.; Thierry, A.; Alfonso, G. C.; Hiltner, A.; Baer, E.; Piorkowska, E.; Galeski, A. *Macromolecules* **2006**, *39*, 5777.
(32) Toki, S.; Sics, I.; Burger, C.; Fang, D.; Liu, L.; Hsiao, B. S.; Datta, S.; Tsou, A. H. *Macromolecules* **2006**, *39*, 3588.
(33) Yave, W.; Quijada, R. *Desalination* **2008**, *228*, 150.
(34) Galland, G. B.; Escher, F. F. N. *Polymer* **2006**, *47*, 2634.
(35) De Rosa, C.; Auriemma, F.; Di Capua, A.; Resconi, L.; Guidotti, S.; Camurati, I.; Nifant'ev, I. E.; Laishevtsev, I. P. *J. Am. Chem. Soc.* **2004**, *126*, 17040.
(36) (a) De Rosa, C.; Auriemma, F.; De Lucia, G.; Resconi, L. *Polymer* **2005**, *46*, 9461. (b) De Rosa, C.; Auriemma, F. *J. Am. Chem. Soc.* **2006**, *128*, 11024. (c) De Rosa, C.; Auriemma, F. *Lect. Notes Phys.* **2007**, *714*, 345.
(37) Ran, S.; Zong, X.; Fang, D.; Hsiao, B. S.; Chu, B.; Phillips, R. A. *Macromolecules* **2001**, *34*, 2569.
(38) Corradini, P.; Petraccone, V.; De Rosa, C.; Guerra, G. *Macromolecules* **1986**, *19*, 2699.
(39) (a) Qamer Zia, Q.; Radusch, H.-J.; Androsch, R. *Polym. Bull.* **2009**, *63*, 755. (b) Androsch, R. *Macromolecules* **2008**, *41*, 533. (c) Mileva, D.; Androsch, R.; Zhuravlev, E.; Schick, C. *Macromolecules* **2009**, *42*, 7275. (d) Mileva, D.; Qamer Zia, Q.; Androsch, R.; Radusch, H.-J.; Piccarolo, S. *Polymer* **2009**, *50*, 5482. (e) Mileva, D.; Androsch, R.; Zhuravlev, E.; Schick, C. *Thermochim. Acta* **2009**, *492*, 67.
(40) Usami, T.; Takayama, S. *Macromolecules* **1984**, *17*, 1756.
(41) Wahner, U. M.; Tincul, I.; Joubert, D. J.; Sadiku, E. R.; Forlini, F.; Losio, S.; Tritto, I.; Sacchi, M. C. *Macromol. Chem. Phys.* **2003**, *204*, 1738.
(42) Kissin, Y. V.; Brandolini, A. J. *Macromolecules* **1991**, *24*, 2632.
(43) (a) Natta, G.; Peraldo, M.; Corradini, P. *Rend. Accad. Naz. Lincei* **1959**, *26*, 14. (b) Natta, G.; Corradini, P. *Nuouo Cimento, Suppl.* **1960**, *15*, 40.
(44) Guerra, G.; Petraccone, V.; De Rosa, C.; Corradini, P. *Makromol. Chem., Rapid Commun.* **1985**, *6*, 573.
(45) Corradini, P.; De Rosa, C.; Guerra, G.; Petraccone, V. *Polymer* **1989**, *30*, 281.
(46) Ungar, G. *Polymer* **1993**, *34*, 2050.
(47) Wunderlich, B.; Grebowicz, J. *Adv. Polym. Sci.* **1984**, *60/61*, 1.
(48) Allegra, G.; Meille, S. V. *Macromolecules* **2004**, *37*, 3487.
(49) Brandrup, J.; Immergut, E. H.; Grulke, E. A. *Polymer Handbook*; John Wiley: New York, 1999.